Triple-Helical Crystalline Structure of Curdlan and Paramylon Hydrates†

Chaw Teo Chuah and Anatole Sarko*

Department of Chemistry, State University of New York, College of Environmental Science and Forestry, Syracuse, New York 13210

Yves Deslandes‡ and Robert H. Marchessault*,‡

Chemistry Department, Université de Montreal, CP 6210, Succ. A, Montreal, Quebec, Canada H3C 3V1. *Received November 3, 1982*

ABSTRACT: The crystal and molecular structure of the hydrated form of (1→3)-β-D-glucan of native curdlan and paramylon has been determined by combined X-ray diffraction and stereochemical model refinement, using data from X-ray fiber diagrams of curdlan and powder diagrams of paramylon. The structure crystallizes as a triplex of right-handed, sixfold helical chains in a hexagonal unit cell with parameters $a = b = 15.56 \pm 0.05$ Å and c (fiber repeat) = 18.78 ± 0.05 Å. The probable space group is $P1$, but the three strands of the triplex are close to $P3$ symmetry. The structure shows evidence of disorder, in that all 18 hydroxymethyl groups of the triplex are in nonequivalent rotational positions, and the locations of water molecules are at least partly random. Of the 36 water molecules present in the unit cell, half appear to be clustered near the O(4) and O(5) atoms of the glucose residues, with about one water for every residue. The other half of the water molecules appear to be distributed in a statistical manner. The conformational characteristics of the chains are very similar to those of the anhydrous form of the structure. The reliability of the structure analysis is indicated by the X-ray residual $R = 0.165$.

Introduction

Curdlan is an extracellular, bacterial polysaccharide that is representative of a class of (1→3)-β-D-glucans that occur in many fungi, bacteria, algae, and plants. It crystallizes easily in two or more polymorphic forms.[1] Its native form, which is usually imperfectly crystalline, readily yields a highly crystalline, hydrated polymorph upon annealing in the presence of water, and upon further annealing under vacuum, converts to an anhydrous crystalline structure. The latter has been shown by X-ray diffraction analysis to be a triplex (three-stranded) structure.[2] The structure of the triplex is stabilized by extensive interstrand and interhelix hydrogen bonds.

In paramylon, the granular form of this polysaccharide extracted from the alga *Euglena gracilis*, the polysaccharide is naturally very highly crystalline and exhibits the diffraction pattern of the hydrated form.[3,4] In view of the differences in the X-ray diffraction diagrams obtained from the anhydrous and the hydrated forms of the polysaccharide, it was of interest to determine whether the natural, hydrated polymorph was also a triplex structure and, if so, whether the two triplexes were similar. The present study was, consequently, undertaken to determine the structure of the hydrated form. As before, X-ray diffraction analysis aided by stereochemical model refinement was used,[2] with diffraction data obtained from both fiber diagrams of curdlan and powder patterns of paramylon.

Experimental Section

The curdlan was obtained from Takeda Chemical Co., Japan, and the paramylon granules were extracted from depigmented *Euglena gracilis* and were gifts from Dr. B. A. Stone of La Trobe University, Australia, and Dr. Miyatake of the Osaka Prefecture University, Japan. When X-ray diffraction diagrams of the as-received samples were recorded, both corresponded to the anhydrous form. An additional sample from Dr. B. A. Stone received via Dr. H. Chanzy of CERMAV, Grenoble, France, was "never dried" and its X-ray diffractogram (recorded with the sample in a sealed capillary) was the hydrate polymorph reported previously.[4] The as-received "dry" samples were convertible to the hydrate by a suitable steam/pressure annealing.[4]

Oriented fibers of curdlan were produced by extruding a 10% solution in dimethyl sulfoxide into a methanol bath at room temperature. The fibers were washed in water and annealed under tension in a sealed bomb at 145 °C in the presence of water.[2]

X-ray fiber patterns and powder patterns were recorded in a flat-film camera at 75% relative humidity; representative diagrams are shown in Figure 1. Note the higher crystallinity and greater line sharpness of paramylon in comparison with curdlan.

The density of the hydrated fibers was measured by flotation in a *p*-xylene–toluene mixture.

The unit cell parameters were determined from the fiber diagram and were then refined by least-squares procedures using 28 observed d spacings. Relative intensities of the reflections in both curdlan and paramylon patterns were obtained from radial tracings of the X-ray films recorded with a Joyce-Loebl microdensitometer. The peak areas under the tracings were resolved into individual intensities with a least-squares curve resolution program.[5] All intensities were corrected for Lorentz and polarization factors, unequal film-to-sample distances of the diffracted rays, and in the case of the fiber diagrams, the arcing of the reflections.[6] The square roots of the corrected, integrated intensities constituted the observed, relative structure factor amplitudes. The structure amplitudes of the unobserved reflections were determined by arbitrarily assigning to them one-half of the minimum observable intensity in the corresponding region of the diffraction angle. For curdlan, a total of 41 observed structure factor amplitudes were obtained in this manner, to which 55 hkl planes contributed. For paramylon, 18 intensities could be measured, to which 41 hkl planes contributed. An additional 38 unobserved structure factor amplitudes were obtained for paramylon. All of the observed reflections in the powder pattern of paramylon were indexed with the help of the fiber pattern of curdlan. The measured and calculated d spacings are shown in Table I.

The structure solution was carried out with the refinement program PS79 using essentially the previously described strategy.[2,7] Steps particular to the refinement methodology of this study are described in conjunction with the results.

Results and Discussion

Unit Cell. As in the case of the anhydrous form, the hydrate structure also crystallizes in a hexagonal lattice, with unit cell dimensions $a = b = 15.56 \pm 0.05$ Å and c (fiber axis) = 18.78 ± 0.05 Å. These dimensions, when compared with those of the anhydrous form ($a = b = 14.41$ Å, $c = 5.87$ Å), show a ca. 8% increase in the base-plane

† Part 14 of the series "Packing Analysis of Carbohydrates and Polysaccharides".

‡ Present address: Xerox Research Centre of Canada, 2480 Dunwin Drive, Mississauga, Ontario, Canada L5L 1J9.

0024-9297/83/2216-1375$01.50/0

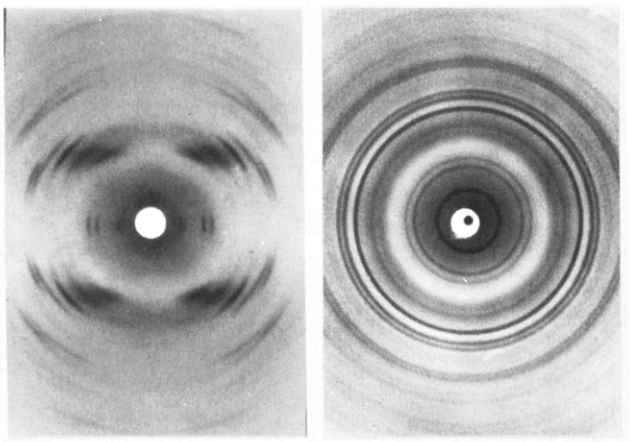

Figure 1. X-ray diffraction diagrams of curdlan hydrate (left) and paramylon (right). Flat film, film-to-sample distance 5 cm. For curdlan hydrate, the fiber axis is vertical.

Table I
Comparison of Calculated and Observed *d* Spacings (Å) for Curdlan Hydrate

hkl	obsd	calcd	*hkl*	obsd	calcd
100	13.60	13.48	125	3.02	3.02
110	7.82	7.78	305	2.87	2.88
200	6.78	6.74	026	2.84	2.84
230	3.10	3.09	126	2.65	2.66
151	2.40	2.40	306	2.56	2.57
222	3.61	3.59	226	2.45	2.44
132	3.47	3.47	326	2.19	2.20
113	4.98[a]	4.87	127	2.36	2.37
203	4.54	4.58	307	2.30	2.30
123	3.93	3.95	028	2.19	2.21
303	3.64	3.65	128	2.12	2.13
124	3.44	3.45	038	2.07	2.08
224	2.99	2.99	228		2.01
134	2.91	2.92	138	1.99	1.99
404	2.72	2.74			

[a] Obscured by amorphous ring; not used for refinement of cell parameters.

dimensions, but a more than threefold increase in the fiber repeat.[2] However, the increase in the latter is simply a manifestation of lower symmetry in the hydrate, compared with the anhydrous form. In the latter, the space group is $P6_3$ and even though each strand of the triplex has a 6_1 conformation with a repeat per turn of 17.61 Å, the consequence of the space group symmetry is that the *c* repeat corresponds to only $^1/_3$ of the full turn of the helix, or 17.61/3 = 5.87 Å, which is equivalent to two anhydroglucopyranose residues. In the hydrate the symmetry is reduced to *P*1 (or *P*3, at best; see later), the consequence of which is that the *c* repeat is now identical with the helix repeat for a full turn.

In addition to the change in the unit cell base plane, the helix repeat of the hydrate has also increased, from a value of 17.61 Å in the anhydrous form to 18.78 Å in the hydrate. The combined increases in the helix repeat and the base-plane dimensions of the unit cell have increased the volume of the unit cell of the hydrate to 3938 Å^3, from the corresponding volume of 3167 Å^3 (for 3 unit cells) in the anhydrous structure, or an increase of ca. 24%. Assuming that the volumes in both cases contain the same number of anhydroglucopyranose residues (a justified assumption, as shown later), considerable space in the hydrate structure must be filled with water. The observed density of curdlan hydrate is 1.47 g/cm^3; the calculated density in closest agreement with this value, assuming the unit cell contains one triplex with a 6_1 chain confirmation or 18 anhydroglucopyranose residues and 36 molecules of water (two water molecules for every glucose residue), is 1.50 g/cm^3. On the other hand, if the molecular conformation of each strand of the triplex was 7_1, as has been suggested elsewhere for curdlan gels,[8] the present structure could not contain any water for the same observed density.

Helix Structure. Based on the similarity of the crystalline lattices of the hydrate and anhydrous structures, the most probable model for the helix structure was, again, a right-handed triplex, composed of three 6_1 strands. A stereochemically sound model for it was easily obtained through packing refinement starting with the coordinates of the anhydrous structure. Because of the increased axial rise per residue and the increased unit cell volume of the hydrate structure, the triplexes were now considerably farther apart and a single best-packing model could not be predicted by the refinement procedure. Neither could a preferred O(6) rotational position be predicted. There was ample space between the triplexes for the water molecules.

The alternative seven-residue model was similarly tested by packing refinement. Even though the conformation of a sevenfold triplex could be easily refined to a good stereochemical state, the increase in its diameter over the sixfold triplex was far too large for the sevenfold triplex to fit into the unit cell and a stereochemically reasonable packing position could not be obtained. Consequently, the sixfold, right-handed triplex remained as the only probable model for the hydrate structure. The comparable left-handed helix was not considered in view of the fact that the transformations between the anhydrous and hydrate forms of the triplex are reversible and occur easily (simply by hydration or dehydration), and the structure does not decrystallize during such transformations.

X-ray Refinements. Initial Structure. Because of the inability to predict reasonable phasing models through packing refinement, the structure had to be solved entirely by X-ray refinement. The structural features that needed to be determined included the final conformations of the individual strands of the triplex (including the O(6) rotations), the packing of the triplexes (i.e., the rotational position of the triple helix in the unit cell), and the location of water molecules. It was hoped that the space group could be determined in the process.

All the steps of the X-ray refinement were carried out with the structure factor amplitudes determined from the powder patterns of paramylon. This data set was used in favor of the amplitudes determined from the fiber diagrams of curdlan, simply because the reflections in the latter were considerably arced and, therefore, subject to measurement error. As shown in Figure 1, the paramylon powder pattern was sharp and well resolved, and all 18 measured reflections could be unambiguously indexed with the help of the fiber patterns.

In the first cycle of refinement, the position of the triplex in the lattice was determined by refinement in projection against 12 *hk*0 reflections, assuming that the structure had $P6_3$ symmetry. The refinable variables were rotation of the triplex about the *c* axis, rotation of the anhydroglucopyranose residue about its *virtual bond*,[23] and the rotation of the O(6) hydroxyl about the C(5)–C(6) bond. The refinement was started at 10° intervals for the rotational position of the triplex between 0° and 60°, and for each starting position three O(6) rotational positions—gt, gg, and tg—were tested.[9] Water was not included in the unit cell during these cycles of refinement, and the refinement criterion was the usual unweighted *R* factor.[10]

It was quickly established that only one packing position of the triplex was a probable one. The results were less

Table II
Characteristics of Models Tested during Refinement

run	space group	residues in asym unit	indep O(6)'s	no. of H_2O's in cell	reflections used	atomic scattering factors	R
5	$P3$	1	1	0	12 $hk0$	ordinary	0.328
5	$P3$	1	1	0	38 hkl, obsd	ordinary	0.424
10	$P3$	1	1	36	38 hkl, obsd	ordinary	0.306
12	$P3$	3	3	36	42 hkl, obsd	ordinary	0.247
19	$P3$	1	1	0	12 $hk0$	H_2O wtd	0.150
26	$P3$	6	6	0	79 hkl, all	H_2O wtd	0.426
25	$P3$	6	6	9	79 hkl, all	H_2O wtd	0.316
23	$P3$	6	6	18	79 hkl, all	H_2O wtd	0.207
24	$P3$	6	6	36	79 hkl, all	H_2O wtd	0.220
35	$P1$	18[a]	18	18	79 hkl, all	H_2O wtd	0.165

[a] $P3$ symmetry for chains, excluding O(6)'s.

clear-cut for the O(6) position, although a slight preference for the O(6)gg position emerged. The R factor for the best structure obtained in this manner was 0.328 (run 5 in Table II), which was reasonably low considering the imposition of higher symmetry. It also ensured that the sixfold, right-handed helix model for the triplex was a correct one. Including the relatively strong $hk3$ and $hk6$ reflections in the refinement (to a total of 38 observed reflections) increased the R factor to 0.424 (run 5 in Table II), which was also not excessive considering that the water was not included.

The presence of weak reflections on layer lines with $l \neq 3n$ indicted, of course, that $P6_3$ symmetry was not present. In order to test whether the lower symmetry was due to changes in the chain conformation, the space group was assumed to be $P3$ and the chain asymmetric unit was taken to contain three anhydroglucopyranose residues. Again, with no water present, the structure was refined against 42 observed $F(hkl)$'s. The refinable variables now included the ring torsion angles for all three residues, three glycosidic bridge angles, three O(6) rotations, and the rotation of the triplex about the c axis. After a few cycles of refinement it became clear that the chain conformation was becoming seriously distorted. Obviously, the lowered symmetry of the hydrate structure was not caused by reasonable changes in chain conformation. Therefore, the only apparent cause for it remained the structure of the water in the unit cell.

Placement of Water. Initial attempts to place the 36 water molecules, indicated to be present by crystalline density, were made with $P3$ symmetry. The triplex conformation was left invariant at that indicated by $P6_3$ symmetry. The 12 independent water molecules were fed into the unit cell one by one, into spaces suggested by a difference Fourier map. These spaces were, as expected, between the triplexes. The rotational position of the triplex and the x, y, z parameters of each water molecule (as oxygen) were refined prior to the addition of another water molecule, and all previously added water molecules were corefined with each newly added water. No attempt was made to eliminate any of the short contacts that developed. This process was repeated many times with different starting positions of the water molecules. In each case, a different result was obtained. A representative result, having an R factor of 0.306, is included in Table II (run 10). Increasing the asymmetric unit to three glucopyranose residues lowered the R factor to 0.247 for 42 observed hkl's and resulted in unequal O(6) rotations for the three residues (run 12 in Table II). However, the model was marked by many short contacts.

The results obtained in this fashion clearly pointed to a structure in which the water molecules did not occupy

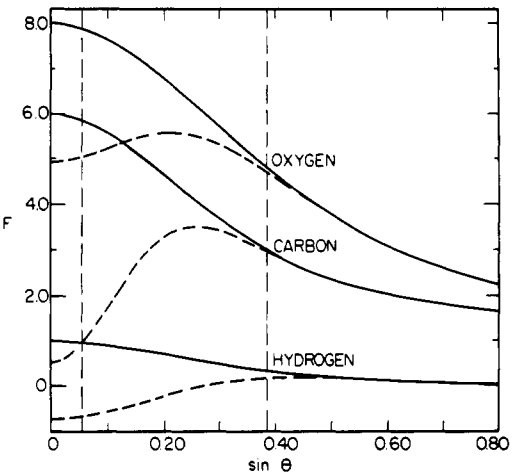

Figure 2. Comparison of normal (solid line) and water-weighted (dashed line) atomic scattering factors for oxygen, carbon, and hydrogen. The vertical dashed lines delimit the range of observed reflections.

well-defined, crystallographic positions. This was not surprising in view of the observation that the water content of the hydrate could be reduced and the structure eventually converted to its anhydrous form simply by evacuation. A different refinement strategy was now adopted employing water-weighted atomic scattering factors.[11] The use of such scattering factors assumes that the volume of the unit cell occupied by water is filled with an electron gas whose density is equal to the mean electron density of the water. The water-weighted atomic scattering factors can be easily calculated[11] and as shown in Figure 2, their functional dependence on sin θ shows considerable differences compared with the ordinary scattering factors, particularly in the range of the reflections observed here. The successful use of the water-weighted scattering factors with some water-containing structures has been documented.[12-14]

As shown in Table II, incorporating the water-weighted atomic scattering factors into the refinement of the simplest model—with 6_1 chain symmetry and $P3$ packing symmetry—immediately reduced the R factor to 0.150 (for 12 $hk0$ reflections and no water in the unit cell; run 19), from a value of 0.328 previously obtained with normal scattering factors. Consequently, all subsequent refinement was carried out with the water-weighted scattering factors. However, it still remained to be determined if some of the water molecules were in preferred positions, as would be expected from their hydrogen-bonding potential. To determine this, a number of refinements were completed with varying amounts of water in the unit cell,

ranging from 0 to 36 molecules. All 79 reflections were used in these refinements in which the space group was $P3$ and the chain backbone conformation was 6_1, but each anhydroglucopyranose residue had an independently rotatable O(6). As shown in Table II for water contents of 0, 9, 18, and 36 molecules per unit cell (runs 23–26), the lowest R factor was obtained for a structure containing 18 water molecules, or one water for each anhydroglucopyranose residue. An increase to a water content of 36 molecules did not decrease the R factor any further. In the refinement process, all six independent O(6) rotations also adopted a different value, distributed as follows: two near gg, two near tg, one near gt, and one halfway between gg and tg. The 18 water molecules encircled the triplex, with roughly one water molecule in the vicinity of each glucose residue and particularly close to the O(4) and O(5) atoms. Many different refinement runs were made attempting to place these water molecules, and although different results were obtained in all cases, a similar encircling of the triplex by water molecules was always found. No apparent symmetry in the water positions (other than the superimposed $P3$ symmetry) was evident, and this, coupled with the variety of O(6) positions, was thought to indicate that the hydrate structure was marked by disorder on the periphery of the triplex.

Final Structure. The final cycles of refinement were carried out by as nearly a complete removal of symmetry as was possible. Each strand of the triplex was considered to be an independent chain, with all 18 glycopyranose residues having independently rotatable O(6) hydroxyls. However, in order not to have an excessive number of refinable variables, the ring portions of all anhydroglucopyranose residues were considered to be identical and the backbones of the three strands of the triplex were still constrained to maintain 6_1 symmetry. The three strands were also still related by $P3$ symmetry—relative to the rings, but not O(6)'s. Refining under these conditions, in $P1$ space group with all 79 reflections, and with the triplex rotation, ring torsion angles of the asymmetric unit, all O(6) rotations, and the positions of 18 water molecules as variables reduced the R factor to 0.165 (weighted R'' = 0.167 with half-weight assigned to all unobserved reflections[10]). Further reduction of $P3$ symmetry, i.e., allowing each strand of the triplex to move independently, produced no further improvement in the R factor. More importantly, it demonstrated that a substantially symmetric triplex structure was being maintained. No further reduction of symmetry—e.g., allowing each glucopyranose ring to flex independently—was tested, as this would have introduced too many variables into the refinement.

The main characteristics of the structure are given in Table III and its hydrogen bonds are listed in Table IV. The conformational characteristics of the chain are unremarkable, with the bridge angle at a reasonable value of 112° and the ϕ(O(5)) angle at −85°. The latter shows a presence of the *exo-anomeric* effect, as expected.[15] The triplex is held together by the same, strong, interstrand O(2)---O(2) hydrogen bonds, 2.77 Å in length, as in the anhydrous structure.[2] Further comparing the features of the anhydrous and hydrate forms shows other similarities. The *virtual bond* lengths are similar in both structures: 4.741 Å in the anhydrous and 4.776 Å in the hydrate. The dihedral angles ϕ and ψ are very similar in both structures, with differences of only 6° and 2° between the respective angles. The similarities extend to the rotational position of the triplex in the unit cell, with a less than 10° difference between the two structures. The main differences are seen on the periphery of the triplexes where the O(6) hydroxyls reside. In the anhydrous form, all O(6)'s are in the tg rotational position, hydrogen bonded to other O(6) and O(4) hydroxyls. In the hydrated structure, all O(6) rotations are different, with seven near the gg position, four not far from the tg position, three near the gt position, and four at intermediate positions (cf. Table III). Despite this apparent randomness, all but three of the 18 O(6) hydroxyls are intertriplex hydrogen bonded to other O(6) and

Table III
Characteristics of the Final Structure

parameter			value		
helix rotation angle,[a] deg			41.5		
glycosidic bridge angle, deg			112.4		
O(6) rotation angles,[b] deg					
$O(6)_1$	$O(6)_7$	$O(6)_{13}$	−77.8	−81.2	−99.9
$O(6)_2$	$O(6)_8$	$O(6)_{14}$	147.9	124.0	145.3
$O(6)_3$	$O(6)_9$	$O(6)_{15}$	116.6	157.4	149.6
$O(6)_4$	$O(6)_{10}$	$O(6)_{16}$	47.4	49.7	59.5
$O(6)_5$	$O(6)_{11}$	$O(6)_{17}$	−62.1	−61.8	−64.3
$O(6)_6$	$O(6)_{12}$	$O(6)_{18}$	−126.0	−95.4	−117.6
length of glucopyranose residue (*virtual bond*),[c] Å				4.776	
conformational torsion angles,[d] deg					
ϕ				35.2	
ϕ(O(5))				−84.5	
ψ				8.4	
packing energy/glucose residue[e] (arbitrary units)				23.1	
X-ray refinement residuals[f]					
R				0.165	
R''				0.167	

[a] Helix rotation is 0° when $O(3)_1$ is at $(0, -y, z)$; positive rotation is clockwise looking down the helix (c) axis. [b] O(6) is at 0° when the bond sequence O(5)-C(5)-C(6)-O(6) is cis and gt = 60°, tg = 180°, and gg = −60°. Atom subscripts indicate residue numbering. $O(3)_i$---$O(3)_{i+1}$. [d] ϕ: $H(1)_1$-$C(1)_1$-$O(3)_2$-$C(3)_2$; ϕ(O(5)): $O(5)_1$-$C(1)_1$-$O(3)_2$-$C(3)_2$; ψ: $C(1)_1$-$O(3)_2$-$C(3)_2$-$H(3)_2$. The angle is 0° when the bond sequence is cis; positive angle is when in sequence A(1)-A(2)-A(3)-A(4) atom A(4) is clockwise relative to A(1), viewing from A(2) to A(3). [e] See ref 7 for the definition of packing energy. [f] See note 10 in references.

Table IV
Hydrogen Bonds of the Final Structure

hydrogen bond	length, Å	hydrogen bond	length, Å
A. Interstrand			
$O(2)_{1-6}$---$O(2)_{7-12}$	2.77	$O(2)_{7-12}$---$O(2)_{13-18}$	2.77
$O(2)_{1-6}$---$O(2)_{13-18}$	2.77		
B. Intertriplex[a]			
$O(4)_1$---$O(6)_{13}^{v}$	3.05	$O(6)_7$---$O(4)_{13}^{iii}$	2.88
$O(6)_1$---$O(4)_7^{i}$	2.86	$O(6)_8$---$O(6)_{14}^{v}$	2.93
$O(6)_2$---$O(6)_{14}^{i}$	2.87	$O(6)_9$---$O(6)_{15}^{i}$	2.81
$O(6)_3$---$O(6)_9^{iv}$	2.87	$O(6)_{11}$---$O(4)_{17}^{iv}$	2.84
$O(4)_5$---$O(6)_{17}^{ii}$	2.84	$O(6)_{12}$---$O(4)_{18}^{ii}$	3.00
$O(6)_5$---$O(4)_{11}^{iii}$	2.84	$O(6)_{12}$---$O(6)_{18}^{ii}$	2.94
$O(6)_6$---$O(6)_{18}^{iii}$	2.63		

C. Distribution of H Bonds Involving Water

water molecule			number of bonds		
W(1)	W(7)	W(13)	1	2	2
W(2)	W(8)	W(14)	1	2	1
W(3)	W(9)	W(15)	2	3	2
W(4)	W(10)	W(16)	3	3	2
W(5)	W(11)	W(17)	2	2	4
W(6)	W(12)	W(18)	3	2	1

[a] Symmetry operations: (i) $x, y-1, z$; (ii) $x, y+1, z$; (iii) $x-1, y, z$; (iv) $x+1, y+1, z$; (v) $x-1, y-1, z$.

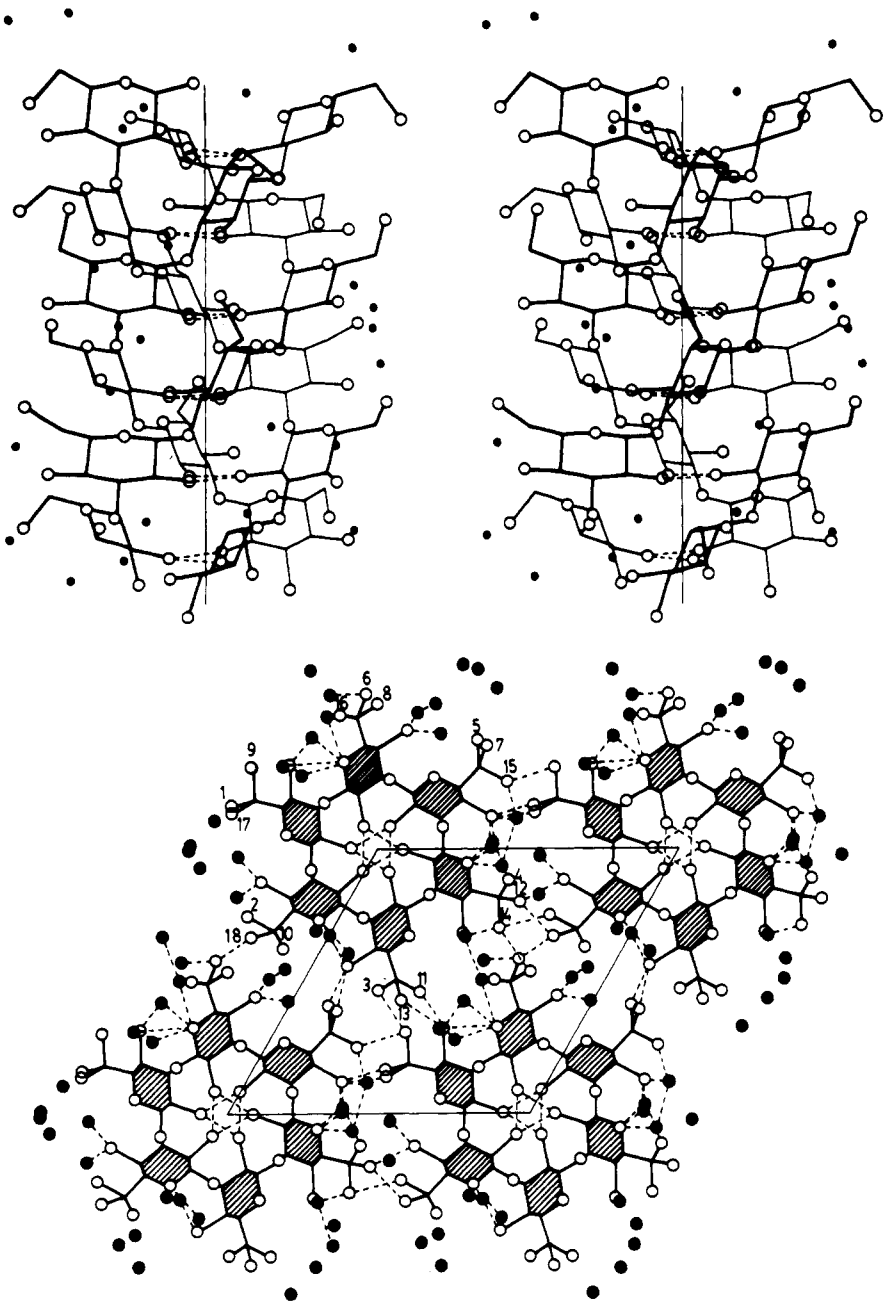

Figure 3. Top: stereoviews of the triplex. Bottom: projection of the crystal structure in the a–b plane. Hydrogen atoms are not shown and water molecules are indicated by filled circles. Hydrogen bonds are drawn with dashed lines. The O(6) atoms of all 18 residues are numbered.

O(4) atoms, in a manner somewhat similar to the anhydrous structure, but without the symmetry of the latter. It also appears (cf. Table III) that despite widely differing rotational positions of the O(6)'s within one chain, there is some similarity between the corresponding residues in the three chains of the triplex. Whether these hydrogen bonds are unique or are representative of a statistical interhelix hydrogen-bond system is not known. Nonetheless, it is clear that the hydrate structure is held together by an extensive network of hydrogen bonds. Likewise, the water molecules appear to contribute in a significant fashion to the hydrogen bonding, despite the apparent randomness of their placement. As shown in Table IV, all 18 water molecules are involved in hydrogen bonds, with the majority of the waters entering into two or more hydrogen bonds. The oxygens most frequently hydrogen bonded to water are the O(4) and O(5) atoms, with only four O(6) atoms bonded in this fashion. Again, it is almost certain that this hydrogen-bond scheme represents a statistically fluctuating system. In all, almost all of the oxygens that are capable of hydrogen bonding in this structure enter into at least one hydrogen bond each. Because of the probable statistical nature of these hydrogen bonds, no attempts were made to refine some of the short hydrogen bonds involving water molecules by imposing stereochemical constraints. Other than some of the short oxygen–oxygen distances among the hydrogen bonds, there were very few short contacts involving other atoms: no interhelix short contacts and only a few moderately short contacts between the water oxygens and some of the helix atoms, principally C(4), H(4), C(6), and the H(6)'s.

The atom coordinates of the final structure are listed in Table V, and the comparison of the calculated and observed structure factor amplitudes is shown in Table VI. A stereoview of the triplex and a projection of the unit cell are shown in Figure 3. (It should be understood that the locations of water molecules as shown in Figure 3 reflect

Table V
Cartesian Atomic Coordinates of Final Structure (A)

atom	X	Y	Z	atom	X	Y	Z
A. Asymmetric Residue[a]				$H(6a)_{10}$	4.843	−5.368	12.060
C(1)	−0.248	−3.380	2.981	$H(6b)_{10}$	3.673	−6.232	12.983
C(2)	−0.593	−2.927	1.572	$O(6)_{11}$	7.174	1.911	15.072
C(3)	−2.088	−2.995	1.369	$H(6a)_{11}$	7.278	0.086	15.984
C(4)	−2.605	−4.390	1.709	$H(6b)_{11}$	6.653	1.351	16.943
C(5)	−2.149	−4.801	3.104	$O(6)_{12}$	2.641	7.053	17.937
C(6)	−2.503	−6.244	3.460	$H(6a)_{12}$	3.420	6.247	19.652
O(2)	−0.129	−1.591	1.357	$H(6b)_{12}$	1.741	6.642	19.709
O(3)	−2.391	−2.701	0.000	$O(6)_{13}$	7.455	1.139	2.294
O(4)	−4.027	−4.409	1.679	$H(6a)_{13}$	7.094	0.198	4.070
O(5)	−0.727	−4.711	3.197	$H(6b)_{13}$	6.626	1.856	3.994
$O(6)_1$	−2.250	−7.125	2.373	$O(6)_{14}$	3.765	6.277	7.300
H(1)	−0.669	−2.725	3.686	$H(6a)_{14}$	1.746	6.654	7.186
H(2)	−0.125	−3.566	0.883	$H(6b)_{14}$	2.592	6.806	5.707
H(3)	−2.557	−2.290	1.989	$O(6)_{15}$	−3.552	6.446	10.341
H(4)	−2.234	−5.077	1.007	$H(6a)_{15}$	−4.842	4.862	10.372
H(5)	−2.581	−4.157	3.811	$H(6b)_{15}$	−4.646	5.591	8.841
$H(6a)_1$	−3.534	−6.287	3.727	$O(6)_{16}$	−6.736	−1.492	14.129
$H(6b)_1$	−1.937	−6.529	4.283	$H(6a)_{16}$	−7.011	−1.645	12.143
B. Hydroxymethyl Groups of All Other Residues[b]				$H(6b)_{16}$	−7.271	−0.081	12.819
				$O(6)_{17}$	−1.979	−7.163	15.041
$O(6)_2$	3.544	−6.426	7.246	$H(6a)_{17}$	−3.565	−6.335	16.026
$H(6a)_2$	4.862	−4.852	7.223	$H(6b)_{17}$	−2.120	−6.451	16.926
$H(6b)_2$	4.629	−5.615	5.711	$O(6)_{18}$	4.425	−6.167	18.011
$O(6)_3$	7.090	0.282	10.920	$H(6a)_{18}$	3.820	−5.863	19.939
$H(6a)_3$	6.700	1.992	9.853	$H(6b)_{18}$	5.039	−4.785	19.364
$H(6b)_3$	7.301	0.682	8.933				
$O(6)_4$	1.852	6.665	13.998	C. Water Molecules			
$H(6a)_4$	2.263	6.873	12.045	W(1)	2.432	−7.252	2.488
$H(6b)_4$	3.555	6.288	13.023	W(2)	7.785	−4.598	5.980
$O(6)_5$	−5.239	5.261	15.068	W(3)	6.735	5.349	10.754
$H(6a)_5$	−3.712	6.259	15.987	W(4)	−1.514	7.192	8.756
$H(6b)_5$	−4.500	5.084	16.942	W(5)	−8.111	6.262	12.899
$O(6)_6$	−7.581	−0.567	18.082	W(6)	−5.694	−3.339	18.967
$H(6a)_6$	−6.939	−0.478	20.015	W(21)	−6.861	2.183	2.029
$H(6b)_6$	−6.689	−1.995	19.234	W(22)	−9.042	−3.306	5.986
$O(6)_7$	−5.000	5.569	2.349	W(23)	0.937	−9.122	10.138
$H(6a)_7$	−3.676	6.187	3.781	W(24)	4.384	−2.482	9.736
$H(6b)_7$	−4.722	4.917	4.244	W(25)	9.160	3.201	12.803
$O(6)_8$	−7.141	−0.149	7.687	W(26)	−0.081	5.849	21.071
$H(6a)_8$	−6.675	−1.969	6.852	W(31)	5.713	5.427	1.571
$H(6b)_8$	−7.282	−0.800	5.757	W(32)	0.406	8.356	5.714
$O(6)_9$	−3.874	−6.324	10.171	W(33)	−9.318	4.555	10.233
$H(6a)_9$	−1.874	−6.577	10.472	W(34)	−3.721	−3.828	7.615
$H(6b)_9$	−2.387	−6.845	8.868	W(35)	−0.194	−9.647	11.845
$O(6)_{10}$	4.811	−4.964	14.026	W(36)	6.138	−4.785	20.493

[a] Other residues of strand 1 are generated by using 6_1 helix symmetry. Strands 2 and 3 are generated from strand 1 by ±120° rotation about the helix axis. [b] Replace coordinates of the hydroxymethyl groups in all but the first (asymmetric) residue. Residues 2-6 are in strand 1, residues 7-12 are in strand 2, and residues 13-18 are in strand 3.

only one of possibly many combinations of water positions.)

Conclusions

The crystal structures of the hydrated and anhydrous forms of the (1→3)-β-D-glucan are very similar—with the dominant feature being the triplex structure. Hydration of it simply expands the lattice, permitting the water to enter the intertriplex spaces. Sixfold helix conformation is maintained and other conformational characteristics of the chains change very little on hydration, other than the apparent removal of constraints on the O(6) rotations. The internal O(2)---O(2) hydrogen bonds are unaffected. Although the water molecules are apparently not in crystallographic positions in the unit cell, half of them (or one water molecule per anhydroglucopyranose residue) tend to cluster around the hydrogen-bonding oxygens in each glucose residue, on the periphery of the triplex.

Because paramylon in its native, hydrated state is highly crystalline, it is probable that its molecular organization into the triplex structure and the subsequent crystallization proceed simultaneously with the biosynthesis of its chains. A parallel exists here with cellulose from *Acetobacter xylinum*, which has been shown to form highly crystalline microfibrils at the time of synthesis.[16] Otherwise, it is difficult to imagine how fully formed, high molecular weight chains could organize into an extensively crystalline triplex structure. On the other hand, even poorly crystalline curdlan fibers can achieve a good level of order upon high-temperature annealing, which seems to indicate that considerable chain mobility may be present even in such constrained structures. The reduced crystallinity of the fibers of curdlan, as compared with paramylon, is almost certainly a consequence of their crystallization from solution. The triplex structure is an all-parallel chain structure, both within the triplex and the lattice packing. Solution crystallization usually favors antiparallel packing, which, in this instance, may occur as flaws in the lattice, thus reducing the degree of crystalline perfection. Calculations[4] based on density determinations have shown that annealed curdlan fibers have a crystallinity of about 40%, while paramylon is at least 80% crystalline.

The physical separation of triplexes on hydration and the consequent rotational freedom of the O(6)

Table VI
Comparison of Calculated and Observed Structure Factor Amplitudes

hkl	*F*(*hkl*)	*F*(calcd) = $[\Sigma F(hkl)^2]^{1/2}$	*F*(obsd)	*hkl*	*F*(*hkl*)	*F*(calcd) = $[\Sigma F(hkl)^2]^{1/2}$	*F*(obsd)
100	168.3	168.3	247.5	213	311.9		
110	107.4	107.4	134.0	123	350.8	469.5	435.9
200	123.5	123.5	129.4				
120	86.1			303	358.6		
210	68.5	110.1	81.0[a]	222	72.5	366.0	390.5
300	120.1	120.1	91.6[a]	223	239.6	239.6	239.2
220	71.8	71.8	71.2[a]				
130	67.8			313	201.8		
310	60.1	90.6	73.4[a]	133	183.9		
400	58.5	58.5	83.3[a]	304	36.3	275.4	222.5
230	120.3			104	48.1	48.1	68.2[a]
320	95.3	153.5	143.8	114	59.6	59.6	68.9[a]
101	44.9	44.9	25.0[a]	204	76.7	76.7	71.9[a]
111	84.6	84.6	56.8[a]	224	179.3		
201	54.7	54.7	45.5[a]	215	129.3		
121	64.9			125	144.5	264.1	332.2
211	96.1	116.0	84.0[a]	404	204.0	204.0	256.6
301	50.2	50.2	62.9[a]	105	58.9	58.9	76.5[a]
221	67.5	67.5	72.7[a]	115	91.8	91.8	82.5[a]
131	58.8			205	60.2	60.2	85.6[a]
311	51.6	78.2	75.7[a]	225	64.6	64.6	106.0[a]
401	82.7	82.7	84.8[a]	106	126.5	126.5	92.4[a]
231	43.9			116	317.1		
321	110.2	118.7	92.4[a]	134	116.4		
141	57.6			314	107.4		
411	90.5	107.4	97.7[a]	305	67.8	360.9	383.7
501	106.8	106.8	104.5[a]	026	203.7	203.7	187.7
331	87.7	87.7	111.3[a]	216	301.6		
241	48.0			126	105.5		
421	95.6	107.0	113.6[a]	107	38.3		
102	20.9	20.9	35.6[a]	135	39.6		
112	55.8	55.8	45.5[a]	315	45.7	327.5	298.2
202	61.5	61.5	50.0[a]	117	73.8		
302	45.6	45.6	68.2[a]	036	220.9	233.0	240.7
124	47.0			151	68.7		
214	183.6			511	113.7		
312	49.7			226	138.3		
132	201.7	281.2	366.3	207	107.0	219.7	218.0
103	171.9	171.9	72.7[a]				
113	371.0	371.0	302.7				
203	352.9						
122	51.0						
212	72.4	363.9	351.9				

[a] Unobserved reflection.

hydroxyls—which apparently has little influence on crystallinity—suggest that the triplex structure could form even when the O(6) hydroxyls are substituted. Examples of such structures are scleroglucan,[17] schizophyllan,[18] and lentinan,[19] all of which have regular or irregular short-branch substitutions on the main-chain O(6) hydroxyls. All of these polysaccharides are crystalline to varying degrees and all show evidence of triplex structure in their X-ray diffraction diagrams.

As a result of the high degree of crystallinity of paramylon, its powder pattern could be used for quantitative refinement. This is of considerable advantage whenever fiber patterns are arced, as they often are. In this instance, because both fiber and powder patterns were well resolved, the latter could be unambiguously indexed and its intensities resolved with the help of the former. The utility of such refinement is indicated by the fact that when the observed powder pattern intensities were completely resolved on the basis of the fiber pattern intensities, the increase in the *R* factor was not large, from 0.165 to 0.247. This increase reflects more the effects of an unreliable, approximate resolution of intensities, rather than possible inaccuracies of structure. Further improvement in powder pattern refinement could probably be realized through the use of the Rietveld method, in which refinement is accomplished by fitting to the entire line profile of the pattern.[20,21]

Acknowledgment. This study was supported by the National Science Foundation (Grants CHE-7727749 and CHE-8107534). The support of the Ministere de l'Education du Quebec and the Natural Sciences and Engineering Research Council of Canada is acknowledged. Dr. T. L. Bluhm of Xerox Research Centre of Canada kindly

provided the powder pattern of the never-dried paramylon as well as stimulating discussion on this subject.

Registry No. Curdlan hydrate, 86391-84-6; paramylon hydrate, 86391-86-8; (1→3)-β-D-glucan, 86391-85-7.

References and Notes

(1) Marchessault, R. H.; Deslandes, Y.; Ogawa, K.; Sundararajan, P. R. *Can. J. Chem.* **1977**, *55*, 300.
(2) Deslandes, Y.; Marchessault, R. H.; Sarko, A. *Macromolecules* **1980**, *13*, 1466.
(3) Barras, D. R.; Stone, B. A. "The Biology of Euglena"; Academic Press: New York, 1969.
(4) Marchessault, R. H.; Deslandes, Y. *Carbohydr. Res.* **1979**, *75*, 231.
(5) Sarko, A. LSQ (Fortran least-squares curve resolution program); SUNY College of Environmental Science and Forestry, Syracuse, NY.
(6) Sarko, A. FIBRXRAY (Fortran X-ray intensity correction program); SUNY College of Environmental Science and Forestry, Syracuse, NY.
(7) Zugenmaier, P.; Sarko, A. In "Fiber Diffraction Methods"; French, A. D., Gardner, K. H., Eds; American Chemical Society: Washington, D.C., 1980; ACS Symp. Ser. No. 141, p 225.
(8) Fulton, W. S.; Atkins, E. D. T. In "Fiber Diffraction Methods"; French, A. D., Gardner, K. H., Eds; American Chemical Society: Washington, D.C., 1980; ACS Symp. Ser. No. 141, p 385.
(9) For the description of gt, gg, and tg terminology, see: Sarko, A.; Marchessault, R. H. *J. Polym. Sci., Part C* **1969**, *28*, 317.
(10) $R = \sum||F_o| - |F_c||/\sum|F_o|$; $R'' = \{[\sum w(||F_o| - |F_c||)^2]/[\sum w|F_o|^2]\}^{1/2}$
(11) Fraser, R. D. B.; MacRae, T. P.; Suzuki, E. *J. Appl. Crystallogr.* **1978**, *11*, 693.
(12) Lee, D. M.; Blackwell, J. *Biopolymers* **1981**, *20*, 2165.
(13) Moorhouse, R.; Winter, W. T.; Arnott, S.; Mayer, M. E. *J. Mol. Biol.* **1977**, *109*, 373.
(14) Winter, W. T., Arnott, S. *J. Mol. Biol.* **1977**, *117*, 761.
(15) Perez, S.; Marchessault, R. H. *Carbohydr. Res.* **1978**, *65*, 114.
(16) Haigler, C. H.; Brown, R. M., Jr.; Benziman, M. *Science (Washington, D.C.)* **1980**, *210*, 903.
(17) Bluhm, T. L.; Deslandes, Y.; Marchessault, R. H. *Carbohydr. Res.* **1982**, *100*, 117.
(18) Yanaki, T.; Norisuye, T.; Fujita, H. *Macromolecules* **1980**, *13*, 1462.
(19) Saito, H.; Ohki, T.; Takasuka, N.; Sasaki, T. *Carbohydr. Res.* **1977**, *58*, 293.
(20) Rietveld, H. M. *J. Appl. Crystallogr.* **1969**, *2*, 65.
(21) Young, R. A.; Lundberg, J. L.; Immirzi, A. In "Fiber Diffraction Methods"; French, A. D., Gardner, K. H., Eds.; American Chemical Society: Washington, D.C., 1980; ACS Symp. Ser. No. 141, p 69.
(22) Sundararajan, P. R.; Marchessault, R. H. *Can. J. Chem.* **1975**, *53*, 3563.
(23) With polysaccharides, modeling of the chain conformation is greatly facilitated by using the *virtual bond* rotation method. Its use, advantages, and a comparison with the ϕ,ψ-rotation method have been described.[7,22]

Ion Binding Properties of Crown Ether Containing Network Polymers

Roger Sinta, Bruce Lamb, and Johannes Smid*

Polymer Research Institute, Chemistry Department, College of Environmental Science and Forestry, State University of New York, Syracuse, New York 13210.

Received November 9, 1982

ABSTRACT: Binding of sodium, potassium, and cesium picrate and of sodium tetraphenylborate to network polymers containing pendant benzo-15-crown-5 and benzo-18-crown-6 ligands was measured spectrophotometrically in dioxane, tetrahydropyran, 2-methyltetrahydrofuran, and tetrahydrofuran as a function of ligand density in the network and the length of the chain connecting the crown ligand with the polystyrene backbone. The immobilized crown ether compounds were synthesized from 2% cross-linked chloromethylated polystyrene containing 0.7, 0.9, and 5 mequiv of Cl/g of polymer. For cation–crown ether combinations yielding only 1:1 complexes the salt binding to the crown network appears to follow Langmuir adsorption behavior close to the point of saturation even for networks containing as much as one crown ligand per two backbone monomer units. Where 1:1 and 2:1 crown–cation complexes can exist (e.g., benzo-15-crown-5 with K^+ or Cs^+ and benzo-18-crown-6 with Cs^+) both 1:1 and 2:1 crown–picrate ion pair complexes appear to exist in the network. A higher crown density in the network favors the 2:1 complexes, but they frequently convert into 1:1 complexes as the salt loading is increased to the point of saturation. Intrinsic binding constants for the picrate salts vary between 10^3 and 4×10^5 M^{-1}, depending on the specific cation–crown combination and the solvent. Increased density of crown ligands in the network invariably enhances the binding constant irregardless of whether 1:1 or 2:1 crown–picrate complexes are formed. Insertion of a $(CH_2)_{10}$ spacer between crown ligand and polystyrene backbone enhances binding constants by less than a factor 2. A change to the more bulky BPh_4 anion increases the binding constant for sodium ion to the benzo-15-crown-5 network in THF by at least a factor 15. The network polymers can also be utilized to measure binding constants of soluble ligands to salts in low-polarity media.

A considerable amount of work has been reported on the properties of polymers containing the cation-chelating crown ethers, cryptands, or podands (e.g., oligooxyethylenes) either as part of the polymer backbone or anchored to the chain as pendant ligands.[1] The use of insoluble supports such as polymeric networks, glass beads, or gels has led to the applications of these ligands as chromatographic stationary phases for separation of both ionic and neutral solutes and as heterogeneous anion-activating catalysts.[2-8] Most studies with immobilized crown ethers or similar ligands have focused on their role in enhancing rates and yields of reactions, especially under phase-transfer conditions, or in evaluating their effectiveness to separate solutes. However, quantitative information on the binding of ionic solutes to crown ether containing network polymers as a function of cation, counterion, solvent, ligand structure or content, and the spacing between polymer backbone and ligand is rather scarce.

This investigation, preliminary data of which were reported in a recent communication,[8] deals with the quantitative measurement of binding constants of alkali picrates

0024-9297/83/2216-1382$01.50/0